

Perfect Core-Shell Octahedral $B@B_{38}^+$, $Be@B_{38}$, and $Zn@B_{38}$ with an Octa-Coordinate Center as Superatoms Following the Octet Rule

Qiao-Qiao Yan,^[a] XiaoYun Zhao,^[b] Ting Zhang,^[a] and Si-Dian Li^{*[a]}

Planar, tubular, cage-like, and bilayer boron clusters $B_n^{+0/-}$ ($n = 3 \sim 48$) have been observed in joint experimental and theoretical investigations in the past two decades. Based on extensive global searches augmented with first-principles theory calculations, we predict herein the smallest perfect core-shell octahedral borospherene $O_h B@B_{38}^+$ (1) and its endohedral metallo-borospherene analogs $O_h Be@B_{38}$ (2), and $O_h Zn@B_{38}$ (3) which, with an octa-coordinate B, Be or Zn atom located exactly at the center, turn out to be the well-defined global minima of the systems highly stable both thermodynamically and dynamically. $B@B_{38}^+$ (1) represents the first boron-containing molecule reported to date which contains an octa-coordinate B center covalently coordinated by eight face-capping boron atoms at

the corners of a perfect cube in the first coordination sphere. Detailed natural bonding orbital (NBO) and adaptive natural density partitioning (AdNDP) bonding analyses indicate that these high-symmetry core-shell complexes $X@B_{38}^{+0/-}$ ($X = B, Be, Zn$) as super-noble gas atoms follow the octet rule in coordination bonding patterns ($1S^2 1P^6$), with one delocalized 9c-2e S-type coordination bond and three delocalized 39c-2e P-type coordination bonds formed between the octa-coordinate X center and its octahedral $O_h B_{38}$ ligand to effectively stabilize the systems. Their IR, Raman, and UV-Vis spectra are computationally simulated to facilitate their spectroscopic characterizations.

Introduction

With the electronic configuration of $[He]2s^2sp^1$, boron exhibits a strong propensity to form multi-center-two-electron (mc-2e) bonds in both its bulk allotropes and polyhedral molecules to compensate for its prototypical electron-deficiency.^[1] At least sixteen distinct bulk allotropes are known to be predominately constructed by three-dimensional icosahedral B_{12} cages that in many cases are accompanied by other interstitial boron atoms lying outside the icosahedrons.^[2] In contrast, joint photoelectron spectroscopy (PES) and first-principles theory studies in the past two decades have unveiled a rich landscape for boron nanoclusters B_n^{-0} from planar or quasi-planar structures ($n = 3 \sim 38, 41 \sim 42$), seashell-like ($n = 28, 29$) and cage-like borospherenes ($n = 39, 40$), to bilayer motifs ($n = 48$), indicating a typical size- and charge-dependent structural evolution in boron nanoclusters.^[3] Meanwhile, combined ion-mobility spectrometry and density functional theory (DFT) investigations showed that B_n^+ monocations possess double-ring cylinder structures in the size range between $n = 16 \sim 25$.^[4] The previously proposed perfect cage-like B_{80} constructed by capping the

twenty hexagons on C_{60} spurred renewed interests in all-boron fullerenes.^[5] The first experimentally observed cage-like B_{40}^{-0} and B_{39}^- have been expanded to the borospherene family B_n^q ($n = 36 \sim 42, q = n \sim 40$) at first-principles theoretical level,^[6] while the bilayer structural motif observed in B_{48}^{-0} has been extended to $B_{48}^- B_{72}$ and $B_{84}^- B_{98}$ at DFT, with a bilayer bottom-up approach proposed for the experimentally observed bilayer $BL-\alpha^+$ borophenes on Ag(111) based on the observed quasi-planar $C_{6v} B_{36}$.^[7] The chemical reactivity and planar precursor of borospherene B_{40} has been discussed in details in a previous report.^[8] Although there have been no core-shell $B_n^{0/+/-}$ clusters observed to date in experiments in the size range with $n = 3 \sim 48$, medium-sized core-shell boron clusters with icosahedral B_{12} cores have received considerable attention in the past decade in theory, aiming to unveil the bottom-up approach from core-shell boron nanoclusters to boron bulk materials. Mononuclear core-shell $B_{68}, B_{74}, B_{80}, B_{84}, B_{96}, B_{100}, B_{101}, B_{102}$, and B_{112} and binuclear core-shell $C_5 B_{180} ((B_{12})_2@B_{156}), C_5 B_{182} ((B_{12})_2@B_{158}),$ and $C_5 B_{184} ((B_{12})_2@B_{160})$ with one or two interconnected icosahedral B_{12} cores at the center have been predicted at DFT, with $C_5 B_{112}$ and $C_5 B_{184}$ being the most stable mononuclear and binuclear species reported so far in the corresponding cluster size ranges in thermodynamics.^[9] To the best of our knowledge, the smallest core-shell boron cluster proposed so far at DFT level is the axially chiral $C_2 B_{46} (B_2@B_{44})$ which contains a B_2 core at the center along the C_2 molecular axis.^[10] The theoretically obtained core-shell $O_h B@B_{38}$ as the second lowest-lying minimum of the doublet neutral at DFT^[11] is expected to be distorted due to Jahn-Teller effect, as discussed in details below. Perfect tetrahedral core-shell $T_d La_4 B_{29}^{0/+/-}$ have also been recently reported in tetrahedral metal-doped boron clusters in theory.^[12]

[a] Dr. Q.-Q. Yan, T. Zhang, Prof. Dr. S.-D. Li
Institute of Molecular Science,
Shanxi University,
030006 Taiyuan, China
E-mail: lisidian@sxu.edu.cn

[b] Dr. X. Zhao
Department of Applied Chemistry
Yuncheng University
044000 Yuncheng, China

Supporting information for this article is available on the WWW under <https://doi.org/10.1002/cphc.202200947>

However, the smallest core-shell bare boron nanocluster with one B atom at the center as the well-defined global minimum of the system still remains unknown to date in both experiments and theory.

Extensive global minimum (GM) searches and first-principles theory calculations performed in this work indicate that the smallest perfect core-shell octahedral borospherene monocation $O_h B@B_{38}^+$ (1) and its endohedral metallo-borospherene neutral analogs $O_h Be@B_{38}$ (2), and $O_h Zn@B_{38}$ (3) are the highly stable global minima of the systems with an octa-coordinate atom at the center which exhibit superatomic behaviors following the octet rule ($1S^21P^6$). These highly stable core-shell species invite experimental characterizations to establish a bottom-up approach from core-shell boron nanoclusters to bulk boron allotropes.

Results and Discussion

Structures and Stabilities

The optimized perfect core-shell octahedral complexes $O_h B@B_{38}^+$ (1), $O_h Be@B_{38}$ (2), and $O_h Zn@B_{38}$ (3) at PBE0/6-311 + G(d) level^[13] as the well-defined GMs of the systems are collectively depicted in Figure 1, with their alternative low-lying isomers summarized in Figure S1(a)–Figure S1(c). These high-symmetry core-shell complexes $X@B_{38}^{+/0}$ with an octa-coordinate boron or metal atom located exactly at the center ($X=B, Be, Zn$) possess the lowest calculated vibrational frequencies of $\nu_{\min}=323.48, 280.14,$ and 170.79 cm^{-1} and large HOMO-LUMO energy gaps of $\Delta E_{\text{gap}}=2.54, 2.79,$ and 2.65 eV , respectively, well indicating that they are true minima of the systems with high chemical stabilities (Table 1). Similar core-shell octahedral complexes $O_h Cd@B_{38}, O_h Hg@B_{38}, O_h Cu@B_{38}^-, O_h Ag@B_{38}^-, O_h$

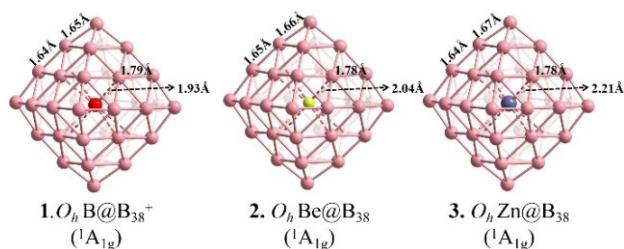


Figure 1. Optimized structures of $O_h B@B_{38}^+$ (1), $O_h Be@B_{38}$ (2), and $O_h Zn@B_{38}$ (3) at PBE0/6-311 + G(d) level, with concerned bond lengths indicated in Å.

$Au@B_{38}^-,$ and $O_h Na@B_{38}^-$ are also obtained which all prove to be the deep-lying minima of the systems without imaginary vibrational frequencies, as collectively shown in Figure S2.

The previously proposed open-shell neutral $O_h B@B_{38}^{[11]}$ proves to be distorted to a doublet $D_{4h} B@B_{38} (^2A_{1g})$ due to Jahn-Teller effect, it is obviously elongated in z-direction along the C_4 main molecular axis. Detachment of one valence electron from it generates the perfect singlet core-shell octahedral monocation $O_h B@B_{38}^+ (1, ^1A_{1g})$ which contains an octa-coordinate B atom as the core located exactly at the center of the octahedral $O_h B_{38}$ shell ligand. The central B in $B@B_{38}^+ (1)$ is mainly coordinated by eight face-capping B atoms in a perfect cube within the first coordination sphere with the B–B coordination bond lengths of $r_{B-B}=1.93\text{ Å}$, as shown in Figure 1. It appears to be the well-defined GM of the monocation lying 0.48, 0.51, 0.55 eV more stable than the second cage-like $C_3 B_{39}^+ (^1A')$,^[14] third triple-ring tubular $C_1 B_{39}^+ (^1A)$, and fourth planar $C_1 B_{39}^+ (^1A)$ at PBE0/6-311 + G(d), respectively (Figure S1(a)), which remains to be confirmed in future gas-phase experiments. The triplet planar $C_1 B_{39}^+ (^3A)$, core-shell $C_1 B@B_{38}^+ (^3A_g)$, and triple-ring tubular $C_1 B_{39}^+ (^3A)$ lie 0.79, 0.80, and 0.92 eV higher than the O_h GM (1). The TPSSh/6-311 + G(d) method^[15] appears to produce approximately the same relative energy orders for the low-lying isomers, as shown in Figure S1(a). Detailed natural bonding orbital (NBO) analyses indicate that the octa-coordinate B in $B@B_{38}^+ (1)$ possesses the net atomic charge of $q_B=+0.13|e|$, electronic configuration of $[He] 2s^{0.51} 2p^{2.26}$, and total Wiberg bond index of $WBI_B=3.78$ (Table 1), with the eight equivalent B–B coordination interactions within the first coordination sphere possessing the covalent bond order of $WBI_{B-B}=0.38$. These results indicate that the central B in $B@B_{38}^+ (1)$ with the total bond order of $WBI_B\approx 4$ is mainly covalently coordinated by eight equivalent face-capping B atoms at the eight corners of an $O_h B_8$ cube, forming a perfect body-centered cubic complex structure in the first coordination sphere. $B@B_{38}^+ (1)$ is the first boron-containing molecule reported to date in chemistry which contains an octa-coordinate B center covalently coordinated by eight boron atoms at the corners of a perfect cube in the first coordination sphere.

Substitution of the central B in $B@B_{38}^+ (1)$ with a Be atom ($[He]2s^2$) generates its isovalent Be-centered octahedral complex $O_h Be@B_{38} (2, ^1A_{1g})$ (Figure 1) which is the deep-lying GM of the metal-doped boron complex with a Be–B coordination bond lengths of $r_{Be-B}=2.04\text{ Å}$. It lies at least 0.88 eV lower than the other low-lying isomers, with the triplet core-shell octahedral $C_{4h} Be@B_{38} (^3A_u)$ lying 1.06 eV higher in energy than the singlet O_h GM (2) at PBE0/6-311 + G(d) (Figure S1(b)). The octa-

Table 1. Calculated lowest vibrational frequencies ν_{\min} , HOMO-LUMO energy gaps (ΔE_{gap}), X–B coordination bond lengths R_{X-B} , total Wiberg bond orders (WBI_X), natural atomic charges (q_X), and electronic configurations of the octa-coordinate X center of $B@B_{38}^+ (1)$, $Be@B_{38} (2)$, and $Zn@B_{38} (3)$ at PBE0/6-311 + G(d).

States	$\nu_{\min}/\text{cm}^{-1}$	$\Delta E_{\text{gap}}/\text{eV}$	$R_{X-B}/\text{Å}$	WBI_{X-B}	$q_X/ e $	Electronic configuration
$B@B_{38}$ $^1A_{1g}$	323.48	2.54	1.93	0.38	0.13	$[He] 2s^{0.51} 2p^{2.26}$
$Be@B_{38}$ $^1A_{1g}$	280.14	2.79	2.04	0.04	1.65	$[He] 2s^{0.26} 2p^{0.08}$
$Zn@B_{38}$ $^1A_{1g}$	170.79	2.65	2.21	0.04	1.73	$[Ar] 3d^{9.96} 4s^{0.27}$

coordinate Be center in Be@B_{38} (2) possesses the net atomic charge of $q_{\text{Be}} = +1.65 |e|$, total bond order of $\text{WBI}_{\text{Be}} = 0.63$, electronic configuration of $[\text{He}] 2s^{0.26} 2p^{0.08}$ (Table 1), and Be–B covalent coordination bond order of $\text{WBI}_{\text{Be-B}} = 0.08$, showing that the less electronegative Be center donates its $2s^2$ valence electrons almost completely to its O_h B_{38} ligand to form a Be^{2+} dication at the center coordinated mainly by electrostatic attractions in a cubic coordination field.

A divalent transition metal Zn atom ($[\text{Ar}]3d^{10}4s^2$) also appears to match the octahedral O_h B_{38} ligand perfectly both geometrically and electronically, as shown in the Zn-centered boron complex O_h Zn@B_{38} (3, $^1A_{1g}$) which, with the Zn–B coordination bond lengths of $r_{\text{Zn-B}} = 2.21 \text{ \AA}$, proves to be the well-defined GM of the neutral complex lying at least 0.46 eV lower in energy than its alternative low-lying isomers. Most of the twenty lowest-lying isomers of ZnB_{38} possess core-shell structures (Figure S1(c)). The octa-coordinate Zn located exactly at the center of Zn@B_{38} (3) possesses the net atomic charge of $q_{\text{Zn}} = +1.73 |e|$, electronic configuration of $[\text{Ar}] 3d^{9.96} 4s^{0.27}$, total bond order of $\text{WBI}_{\text{B}} = 0.67$ (Table 1), and Zn–B covalent coordination bond order of $\text{WBI}_{\text{Be-B}} = 0.08$. These calculated data show that the Zn center donates its $4s^2$ almost completely to the B_{38} ligand and forms mainly electrostatic coordination interactions with the first cubic coordination sphere.

Extensive Born-Oppenheimer molecular dynamics (BOMD) simulations using the CP2K software^[16] on O_h B@B_{38}^+ (1) at 1000 K and O_h Be@B_{38} (2) and O_h Zn@B_{38} (3) at 1200 K in Figure S3 clearly indicate that these core-shell octahedral complexes are all highly dynamically stable at high temperatures, as evidenced by the small calculated average root-mean-square-deviations of $\text{RMSD} = 0.12, 0.14, \text{ and } 0.14 \text{ \AA}$ and the maximum bond length deviations of $\text{MAXD} = 0.46, 0.53, 0.51 \text{ \AA}$, respectively. The core-shell octahedral structures of these complexes are all well maintained during BOMD simulations in 30 ps, with no other low-lying isomers observed.

Bonding Analyses

To better comprehend the high stabilities of these core-shell octahedral borospherene complexes, detailed canonical molecular orbitals (CMOs) and adaptive natural density partitioning (AdNDP)^[17] bonding analyses are comparatively performed on B@B_{38}^+ (1), Be@B_{38} (2), and Zn@B_{38} (3) in Figure 2 and Figure S4. As shown in Figure 2(a), B@B_{38}^+ (1) possesses 24 equivalent 3c-2e σ bonds on six B_9 quadrangular pyramids at the six corners of the octahedral complex with the occupation numbers of $\text{ON} = 1.93 |e|$, 24 equivalent 3c-2e B–B σ bonds on the eight triangular surfaces with $\text{ON} = 1.87 |e|$, and 6 equivalent 9c-2e π bonds on the six B_9 quadrangular pyramids at the corners with $\text{ON} = 1.88 |e|$ in the first row, forming the delocalized σ -skeleton and π -skeleton on the B_{38} ligand in an overall symmetry of O_h . The remaining four delocalized coordination bonds involving the central B atom are classified into two groups, including 1 9c-2e S-type bond with $\text{ON} = 1.91 |e|$ and 3 equivalent 39c-2e P-type bonds with $\text{ON} = 2.00 |e|$. B@B_{38}^+ (1) thus behaves like a super-noble gas atom following the octet rule with the

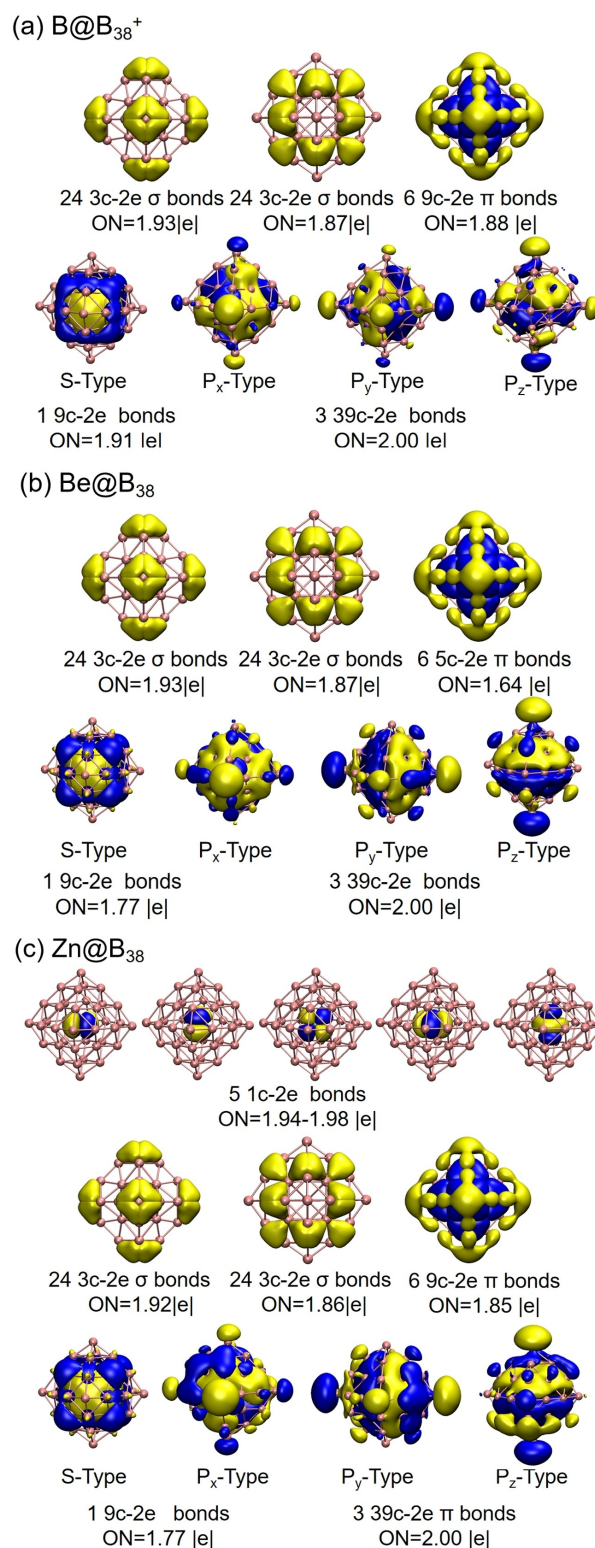


Figure 2. AdNDP bonding patterns of (a) B@B_{38}^+ (1), (b) Be@B_{38} (2), and (c) Zn@B_{38} (3).

electronic configuration of $1s^2 1p^6$. Interestingly, the 1 9c-2e S-type bond and 3 39c-2e P-type bonds of B@B_{38}^+ (1) involving the octa-coordinate B center well correspond to the non-

degenerate S-type HOMO-15 (a_{1g}) and triply degenerate P-type HOMO-2 (t_{1u}) of the complex shown in Figure S4(a).

As expected, the isovalent neutral Be@B_{38} (2) exhibits a similar bonding pattern (Figure 2(b)) with B@B_{38}^+ (1). It has 24 3c-2e σ bonds around the six quadrangular pyramids and 24 3c-2e σ bonds on eight triangular faces to form the σ -skeleton and 6 9c-2e π bonds over the six corners to form the π -skeleton on the B_{38} ligand. The remaining eight valence electrons involving the octa-coordinate Be center are distributed in 1 9c-2e S-type bond and 3 3c-2e P-type bonds of the system, again matching the octet rule [$1S^21P^6$] of a super-noble gas atom. Such a coordination bonding pattern originates from the non-degenerate S-type HOMO-12 (a_{1g}) and triply degenerate P type HOMO-1 (t_{1u}) of the complex, as demonstrated in Figure S4(b).

Zn@B_{38} (3) with a transition metal center possesses a slightly different coordination bonding scheme, as indicated in Figure 2(c). It contains 5 1c-2e d-type lone pairs on the Zn center in the first row and 24 3c-2e σ bonds on six quadrangular pyramids, 24 3c-2e σ bonds six triangular faces, and 6 9c-2e π bonds over six corners on the B_{38} shell in the second row. The 1 9c-2e S-type coordination bond and 3 P-type coordination bonds in the third row involving the octa-coordinate Zn center can be traced back to the non-degenerate HOMO-13 (a_{1g}) and triply degenerate HOMO (t_{1u}) of the complex (Figure S4(c)). It therefore can also be viewed as a super-noble gas atom following the octet rule in the electronic configuration of $1S^21P^6$.

Such superatomic coordination bonding patterns render spherical aromaticity and extra stability to B@B_{38}^+ (1), Be@B_{38} (2), and Zn@B_{38} (3), as evidenced by their calculated isoschemical shielding surfaces (ICSSs)^[18] based on the ZZ components of the calculated nuclear-independent chemical shifts^[19] (NICS-ZZ) depicted in Figure 3. The chemical shielding areas with negative NICS-ZZ values cover the entire space inside the octahedral complexes or within about 1.0 Å above the cage surface in the vertical direction (highlighted in yellow), while the chemical de-shielding areas with positive NICS-ZZ values are mainly distributed in belt-like areas on the waist of the core-shell systems in the horizontal direction (highlighted in green),

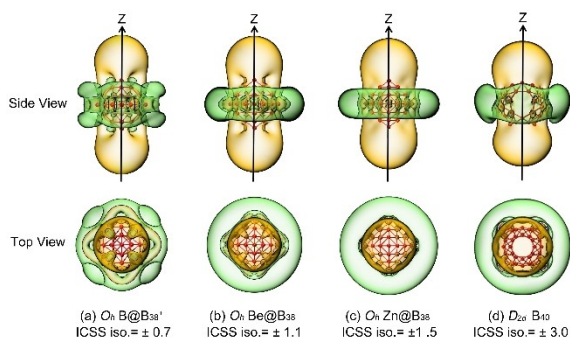


Figure 3. Calculated ICSS surfaces of $O_h \text{B@B}_{38}^+$ (1), $O_h \text{Be@B}_{38}$ (2), and $O_h \text{Zn@B}_{38}$ (3) in comparison with that of $D_{2d} \text{B}_{40}$, with the corresponding NICS-ZZ components indicated. Yellow regions stand for chemical shielding areas, while green areas represent chemical de-shielding areas.

similar to the situation in the experimentally known spherical aromatic $D_{2d} \text{B}_{40}$ as indicated in Figure 3.

Spectral Simulations

The infrared (IR), Raman, and UV-vis spectra of $O_h \text{B@B}_{38}^+$ (1), Be@B_{38} (2), and $O_h \text{Zn@B}_{38}$ (3) are computationally simulated in Figure 4 to facilitate their experimental characterizations. As shown in Figure 4(a), B@B_{38}^+ (1) exhibits three strong IR active peaks at 562 (t_{1u}), 661 (t_{1u}), and 883 (t_{1u}) cm^{-1} and three major Raman scattering peaks at 462 (a_{1g}), 638 (a_{1g}), and 928 (e_g) cm^{-1} , respectively, with the 462 cm^{-1} peak corresponding to typical “radial breathing mode” (RBM)^[20] of the complex which can be used to characterize hollow boron nanostructures. Its simulated UV-Vis spectrum exhibits strong absorption peaks at 216 and 340 nm. There exist two strong IR peaks at 897 (t_{1u}) and 1172 (t_{1u}) cm^{-1} , six major Raman peaks at 314 (e_g), 364 (t_{2g}), 564 (t_{2g}), 619 (a_{1g}), 909 (e_g), and 1179 (a_{1g}) cm^{-1} , and four major UV-vis bands centered around 223, 322, 458, and 547 nm in Be@B_{38} (2) in Figure 4(b). The transition metal-doped Zn@B_{38} (3) exhibits three major IR vibrational modes at 879 (t_{1u}), 931 (t_{1u}), and 1161 (t_{1u}) cm^{-1} , three Raman active vibrations at 344 (t_{2g}), 596 (a_{1g}), and 886 (e_g) cm^{-1} , and two major UV-vis absorptions at 225 and 312 nm, respectively (Figure 4(c)).

Conclusion

Extensive global searches and first-principles theory calculations executed in this work predict the viable possibility of the smallest perfect core-shell octahedral borospherene B@B_{38}^+ (1) and its endohedral metallo-borospherene analogs Be@B_{38} (2) and Zn@B_{38} (3) with an octa-coordinate center which are all the well-defined global minima of the systems as superatoms following the octet rule ($1S^21P^6$) in coordination bonding patterns. These high-symmetry core-shell boron complexes with an octa-coordinate B, Be, or Zn atom located exactly at the center turn out to be spherically aromatic in nature and highly stable both thermodynamically and dynamically. These novel high-symmetry species are expected to be synthesized and characterized in gas-phase experiments via laser ablation of mixed boron targets to enrich the chemistry of boron. They may also serve as building blocks to form low-dimensional nano-materials based in boron clusters, similar to the situations in the previously reported B_6 and B_{20} .^[21]

Computational Procedures

Extensive GM searches on B_{39}^+ , BeB_{38} , and ZnB_{38} were performed at PBE/DZVP level employing the TGMIn program,^[22] in conjunction with manual structural constructions based on related previously reported boron nanoclusters, with more than 1500 isomers probed on the potential energy surface for each species. The seven lowest-lying isomers were then fully reoptimized at both PBE0 and TPSSH levels with the basis set of 6-311+G(d),^[13,15] with frequencies checked to make sure the obtained structures are true minima of

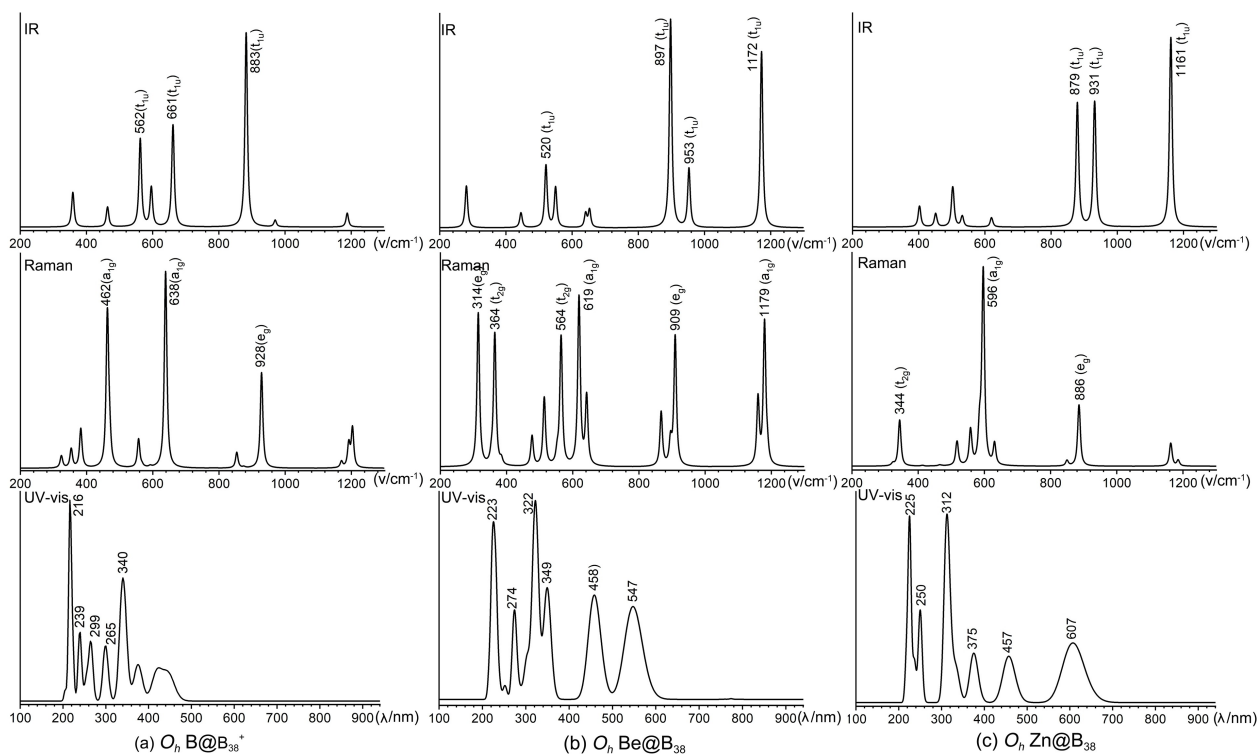


Figure 4. Simulated IR, Raman, and UV-Vis spectra of (a) $B@B_{38}^+$ (1), (b) $Be@B_{38}$ (2), and (c) $Zn@B_{38}$ (3) at PBE0/6-311+G(d).

the systems. Detailed AdNDP bonding analysis^[17] were performed on the ground-state $B@B_{38}^+$ (1), $Be@B_{38}$ (2), and $Zn@B_{38}$ (3). Their iso-chemical shielding surfaces (ICSSs)^[18] were calculated based on the ZZ components of the calculated nuclear-independent chemical shifts^[18] to probe the spherical aromaticity of the systems employing the Multiwfn 3.7 code^[23] and visualized using the visual molecular dynamics (VMD) software.^[24] The infrared and Raman spectra of the core-shell octahedral complexes were simulated at PBE0/6-311+G(d) and their UV-vis spectra calculated using the time-dependent DFT approach^[25] at same theoretical level. All the calculations in this work were done using the Gaussian 09 suite.^[26] Extensive BOMD simulations were performed on 1–3 for 30 ps at different temperatures using the CP2K code, with the GTH-PBE pseudopotential and DZVP-MOLOPT-SR-GTH basis set.^[16]

Acknowledgements

This work was supported by the National Natural Science Foundation of China (21720102006 and 21973057 to S.-D. L.).

Conflict of Interest

The authors declare no conflict of interest.

Data Availability Statement

The data that support the findings of this study are available in the supplementary material of this article.

Keywords: boron nanoclusters · density functional theory · bonding · superatoms · octet rule

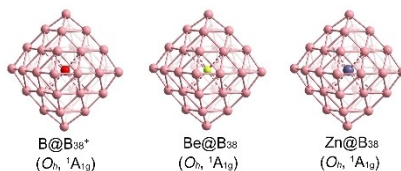
- [1] F. A. Cotton, G. Wilkinson, C. A. Murillo, M. Bochmann, in *Advanced Inorganic Chemistry*, Wiley-Interscience, 6th edition, New York, 1998.
- [2] a) A. R. Oganov, J. H. Chen, C. Gatti, Y. Z. Ma, C. W. Glass, Z. X. Liu, T. Yu, O. O. Kurakevych, V. L. Solozhenko, *Nature* **2009**, *457*, 863–867; b) B. Albert, H. Hillebrecht, *Angew. Chem. Int. Ed.* **2009**, *48*, 8640–8668; *Angew. Chem.* **2009**, *121*, 8794–8824.
- [3] a) L. S. Wang, *Int. Rev. Phys. Chem.* **2016**, *35*, 69–142; b) T. Jian, X. N. Chen, S. D. Li, A. I. Boldyrev, J. Li, L. S. Wang, *Chem. Soc. Rev.* **2019**, *48*, 3550–3591; c) H. Bai, T. T. Chen, Q. Chen, X. Y. Zhao, Y. Y. Zhang, W. J. Chen, W. L. Li, L. F. Cheung, B. Bai, J. Cavanagh, W. Huang, S. D. Li, J. Li, L. S. Wang, *Nanoscale* **2019**, *11*, 23286–23295; d) H. J. Zhai, Y. F. Zhao, W. L. Li, Q. Chen, H. Bai, H. S. Hu, Z. A. Piazza, W. J. Tian, H. G. Lu, Y. B. Wu, Y. W. Mu, G. F. Wei, Z. P. Liu, J. Li, S. D. Li, L. S. Wang, *Nat. Chem.* **2014**, *6*, 727–731; e) Q. Chen, W. L. Li, Y. F. Zhao, H. S. Hu, H. Bai, H. R. Li, W. J. Tian, H. G. Lu, H. J. Zhai, S. D. Li, L. S. Wang, *ACS Nano* **2015**, *9*, 754–760; f) W. J. Chen, Y. Y. Ma, T. T. Chen, M. Z. Ao, D. F. Yuan, Q. Chen, X. X. Tian, Y. W. Mu, S. D. Li, L. S. Wang, *Nanoscale* **2021**, *13*, 3868–3876.
- [4] E. Oger, N. R. Crawford, R. Kelting, P. Weis, M. M. Kappes, R. Ahlrichs, *Angew. Chem. Int. Ed.* **2007**, *46*, 8503–8506; *Angew. Chem.* **2007**, *119*, 8656–8659.
- [5] a) N. G. Szwacki, A. Sadrzadeh, B. I. Yakobson, *Phys. Rev. Lett.* **2007**, *98*, 166804; b) *Nature* **2007**, *447*, 4–5.
- [6] a) W. J. Tian, Q. Chen, H. R. Li, M. Yan, Y. W. Mu, H. G. Lu, H. J. Zhai, S. D. Li, *Phys. Chem. Chem. Phys.* **2016**, *18*, 9922–9926; b) H. Liu, Y. W. Mu, S. D. Li, *J. Cluster Sci.* **2022**, *33*, 81–87; c) Q. Chen, S. Y. Zhang, H. Bai, W. J. Tian, T. Gao, H. R. Li, C. Q. Miao, Y. W. Mu, H. G. Lu, H. J. Zhai, S. D. Li, *Angew. Chem. Int. Ed.* **2015**, *54*, 8160–8164; *Angew. Chem.* **2015**, *127*, 8278–8282.
- [7] a) L. Pei, Q. Q. Yan, S. D. Li, *Eur. J. Inorg. Chem.* **2021**, 2618–2624; b) Q. Q. Yan, L. Pei, S. D. Li, *J. Mol. Model.* **2021**, *27*, 364; c) Q. Q. Yan, T. Zhang, Y. Y. Ma, Q. Chen, Y. W. Mu, S. D. Li, *Nanoscale*

- 2022, 14, 11443–11451; d) Y. Y. Ma, X. Y. Zhao, W. Y. Zan, Y. W. Mu, Z. H. Zhang, S. D. Li, *Nano Res.* **2022**, 15, 5752–5757.
- [8] Y. Yang, Z. Zhang, E. S. Peneva, B. I. Yakobson, *Nanoscale* **2017**, 9, 1805–1810.
- [9] a) D. L. Prasad, E. D. Jemmis, *Phys. Rev. Lett.* **2008**, 100, 165504; b) H. Li, N. Shao, B. Shang, L. F. Yuan, J. Yang, X. C. Zeng, *Chem. Commun.* **2010**, 46, 3878–3880; c) J. J. Zhao, L. Wang, F. Y. Li, Z. F. Chen, *J. Phys. Chem. A* **2010**, 114, 9969–9972; d) L. W. Sai, X. Wu, F. Y. Yu, *Phys. Chem. Chem. Phys.* **2022**, 24, 15687–15690; e) F. Y. Li, P. Jin, D. E. Jiang, L. Wang, S. B. Zhang, J. J. Zhao, Z. F. Chen, *J. Chem. Phys.* **2012**, 136, 074302; f) L. W. Sai, X. Wu, N. Gao, J. J. Zhao, R. B. King, *Nanoscale* **2017**, 9, 13905–13909; g) M. Zhang, H. G. Lu, S. D. Li, *Nano Res.* **2021**, 14, 4719–4724; h) M. Zhang, W. P. Jia, T. Zhang, B. B. Pei, J. Xu, X. X. Tian, H. G. Lu, S. D. Li, *Sci. Rep.* **2022**, 12, 19741.
- [10] L. W. Sai, X. Wu, N. Gao, J. J. Zhao, R. Bruce Kin, *Nanoscale* **2017**, 37, 13905–13909.
- [11] X. Wu, L. W. Sai, S. Zhou, P. W. Zhou, M. D. Chen, M. Springborg, J. J. Zhao, *Phys. Chem. Chem. Phys.* **2020**, 22, 12959.
- [12] X. Q. Lu, C. Y. Gao, Z. H. Wei, S. D. Li, *J. Mol. Model.* **2021**, 27, 130.
- [13] a) C. Adamo, V. Barone, *J. Chem. Phys.* **1999**, 110, 6158–6170; b) R. Krishnan, J. S. Binkley, R. Seeger, J. A. Pople, *J. Chem. Phys.* **1980**, 72, 650–654.
- [14] X. Y. Zhao, Q. Chen, H. R. Li, *Phys. Chem. Chem. Phys.* **2017**, 19, 10998–11003.
- [15] V. N. Staroverov, G. E. Scuseria, J. Tao, J. P. Perdew, *J. Chem. Phys.* **2003**, 119, 12129–12137.
- [16] J. VandeVondele, M. Krack, F. Mohamed, M. Parrinello, T. Chassaing, J. Hutter, *Comput. Phys. Commun.* **2005**, 167, 103–128.
- [17] a) D. Y. Zubarev, A. I. Boldyrev, *Phys. Chem. Chem. Phys.* **2008**, 10, 5207–5217; b) D. Y. Zubarev, A. I. Boldyrev, *J. Org. Chem.* **2008**, 73, 9251–9258; c) N. V. Tkachenko, A. I. Boldyrev, *Phys. Chem. Chem. Phys.* **2019**, 21, 9590–9596.
- [18] a) S. Klod, E. Kleinpeter, *J. Chem. Soc. Perkin Trans. 2* **2001**, 1893–1898;  Dear Author, if the journal has volumes, please add the journal number  b) E. Kleinpeter, S. Klod, A. Koch, *J. Mol. Struct.* **2007**, 811, 45–60.
- [19] a) P. v. R. Schleyer, C. Maerker, A. Dransfeld, H. Jiao, N. J. van Eikema Hommes, *J. Am. Chem. Soc.* **1996**, 118, 6317–6318; b) Z. Chen, C. S. Wannere, C. Corminboeuf, R. Puchta, P. V. R. Schleyer, *Chem. Rev.* **2005**, 105, 3842–3888.
- [20] D. Ciuparu, R. F. Klie, Y. M. Zhu, L. Pfefferle, *J. Phys. Chem. B* **2004**, 108, 3967–3969.
- [21] a) X. F. Zhou, A. R. Oganov, Z. Wang, I. A. Popov, A. I. Boldyrev, H. T. Wang, *Phys. Rev. B* **2016**, 93, 085406; b) N. V. Tkachenko, D. Steglenko, N. Fedik, N. M. Boldyreva, R. M. Minyaev, V. I. Minkin, A. I. Boldyrev, *Phys. Chem. Chem. Phys.* **2019**, 21, 19764–19771.
- [22] a) J. P. Perdew, K. Burke, M. Ernzerhof, *Phys. Rev. Lett.* **1996**, 77, 3865; b) Y. Zhao, X. Chen, J. Li, *Nano Res.* **2017**, 10, 3407–3420.
- [23] T. Lu, F. Chen, *J. Comput. Chem.* **2012**, 33, 580–592.
- [24] W. Humphrey, A. Dalke, K. Schulten, *J. Mol. Graphics* **1996**, 14, 33–38.
- [25] a) R. Bauernschmitt, R. Ahlrichs, *Chem. Phys. Lett.* **1996**, 256, 454–464; b) M. E. Casida, C. Jamorski, K. C. Casida, D. R. Salahub, *J. Chem. Phys.* **1998**, 108, 4439–4449.
- [26] Gaussian 09 (Revision D.01), M. J. Frisch, G. W. Trucks, H. B. Schlegel, G. E. Scuseria, M. A. Robb, J. R. Cheeseman, G. Scalmani, V. Barone, G. A. Petersson, H. Nakatsuji, X. Li, M. Caricato, A. V. Marenich, J. Bloino, B. G. Janesko, R. Gomperts, B. Mennucci, H. P. Hratchian, J. V. Ortiz, A. F. Izmaylov, J. L. Sonnenberg, D. Williams-Young, F. Ding, F. Lipparini, F. Egidi, J. Goings, B. Peng, A. Petrone, T. Henderson, D. Ranasinghe, V. G. Zakrzewski, J. Gao, N. Rega, G. Zheng, W. Liang, M. Hada, M. Ehara, K. Toyota, R. Fukuda, J. Hasegawa, M. Ishida, T. Nakajima, Y. Honda, O. Kitao, H. Nakai, T. Vreven, K. Throssell, J. A. Montgomery, Jr., J. E. Peralta, F. Ogliaro, M. J. Bearpark, J. J. Heyd, E. N. Brothers, K. N. Kudin, V. N. Staroverov, T. A. Keith, R. Kobayashi, J. Normand, K. Raghavachari, A. P. Rendell, J. C. Burant, S. S. Iyengar, J. Tomasi, M. Cossi, J. M. Millam, M. Klene, C. Adamo, R. Cammi, J. W. Ochterski, R. L. Martin, K. Morokuma, O. Farkas, J. B. Foresman, D. J. Fox, Gaussian, Inc., Wallingford, CT, **2009**.

Manuscript received: December 23, 2022
Revised manuscript received: January 26, 2023
Accepted manuscript online: January 30, 2023
Version of record online:  

RESEARCH ARTICLE

Extensive global minimum searches augmented with first-principles theory calculations predict the smallest perfect core-shell octahedral borospherene O_h $B@B_{38}^+$ and its endohedral metallo-borospherene analogs O_h $Be@B_{38}$ and O_h $Zn@B_{38}$ which, as super-noble gas atoms, follow the octet rule and are spherically aromatic in nature.



Dr. Q.-Q. Yan, Dr. X. Zhao, T. Zhang,
Prof. Dr. S.-D. Li*

1 – 7

Perfect Core-Shell Octahedral
 $B@B_{38}^+$, $Be@B_{38}$, and $Zn@B_{38}$ with an
Octa-Coordinate Center as Supera-
toms Following the Octet Rule



 ## SPACE RESERVED FOR IMAGE AND LINK

Share your work on social media! *ChemPhysChem* has added Twitter as a means to promote your article. Twitter is an online microblogging service that enables its users to send and read short messages and media, known as tweets. Please check the pre-written tweet in the galley proofs for accuracy. If you, your team, or institution have a Twitter account, please include its handle @username. Please use hashtags only for the most important keywords, such as #catalysis, #nanoparticles, or #proteindesign. The ToC picture and a link to your article will be added automatically, so the **tweet text must not exceed 250 characters**. This tweet will be posted on the journal's Twitter account (follow us @ChemPhysChem) upon publication of your article in its final (possibly unpaginated) form. We recommend you to re-tweet it to alert more researchers about your publication, or to point it out to your institution's social media team.

ORCID (Open Researcher and Contributor ID)

Please check that the ORCID identifiers listed below are correct. We encourage all authors to provide an ORCID identifier for each coauthor. ORCID is a registry that provides researchers with a unique digital identifier. Some funding agencies recommend or even require the inclusion of ORCID IDs in all published articles, and authors should consult their funding agency guidelines for details. Registration is easy and free; for further information, see <http://orcid.org/>.

Dr. Qiao-Qiao Yan
Dr. XiaoYun Zhao
Ting Zhang
Prof. Dr. Si-Dian Li <http://orcid.org/0000-0001-5666-0591>